Electronic Supplementary Information

$[Sn_3OF]PO_4$ vs $[Sn_3F_3]PO_4$: Enhancing Birefringence through Breaking *R*3 Symmetry and Realigning Lone Pairs

Yuhan Hu[a,b], Xi Xu[a], Ruixi Wang[a], Shunsong Zhang[a], Jingyun Han[a], Shuhui Zhan[a], Jingyu Guo[a,b*], Li-ming Wu[a,b*] and Ling Chen[a,b*]

[a]Center for Advanced Materials Research, Beijing Normal University, Zhuhai 519087, People's Republic of China

[b]Beijing Key Laboratory of Energy Conversion and Storage Materials, College of Chemistry, Beijing Normal University, Beijing, 100875,People's Republic of China

* Corresponding author: jyguo@bnu.edu.cn; wlm@bnu.edu.cn; chenl@bnu.edu.cn

Table of Contents

Supplementary Experimental Section

Synthesis of $[Sn_3F_3]PO_4$

The reagents including SnF_2 (Bldepham, 99 %) and H_3PO_4 (Aladdin, 99 %) were used as purchased. The crystal and polycrystalline powders of $[Sn_3F_3]PO_4$ was obtained in an aqueous solution[1]: 7.05g SnF_2 are dissolved in 40 ml deionized water at 40 °C. The clear solution (previously filtered if some turbidity is present) is heated up to 50 °C and 15 ml H_3PO_4 (1mol/L) is added dropwise under continuous stirring. The colourless block-like $[Sn_3F_3]PO_4$ microcrystalline is filtered from the yet warm solution, washed with a small amount of deionized water and ethanol, finally dried at 70 °C during 12 h, and the yield of $[Sn_3F_3]PO_4$ product is 100% without impurity.

Electron Dispersive Spectroscopy

$[Sn_3OF]PO_4$ and $[Sn_3F_3]PO_4$ crystals surfaces were characterized by electron dispersive spectroscopy (EDS) using a JMS-7610FPlus scanning electron microscope (SEM), equipped with an Oxford X-MasN EDS detector with a 20 mm^2 window, operated with an accelerating voltage of 20 kV and a working distance of 10 mm.

Second Harmonic Generation Response

Powder SHG was measured using the Kurtz and Perry method[2] with Q-switched Nd: YAG lasers at wavelengths of 1064 nm. Polycrystalline $[Sn_3F_3]PO_4$ samples were ground and sieved into a series of distinct size ranges, namely, 30–45, 45–75, 75–109, 109–150, and 150–212 μm, and KDP sieved into the same size ranges were used as references.

Table S1. Crystal data and structure refinement for $[Sn_3OF]PO_4$ and $[Sn_3F_3]PO_4$.

Empirical formula	$[Sn_3OF]PO_4$	$[Sn_3F_3]PO_4$	$[Sn_3F_3]PO_4$[#1]
Formula weight	486.04	508.04	508.04
Temperature	300.0 K	302.0 K	100 K
Wavelength	0.71073 Å	0.71073 Å	0.71073 Å
Crystal system	Monoclinic	Trigonal	Trigonal
Space group	$P2_1/c$	$R3$	$R3$
Unit cell dimensions	a = 4.8865(2) Å	a = 11.8537(3) Å	a = 11.8096(4) Å
	b = 11.4484(5) Å	b = 11.8537(3) Å	b = 11.8096(4) Å
	c = 11.9947(5) Å	c = 4.6271(2) Å	c = 4.65010(10)
	α = 90 °	α = 90 °	α = 90 °
	β = 97.286(1) °	β = 90 °	β = 90 °
	γ = 90°	γ = 120°	γ = 120°
Volume	665.60(5) Å^3	563.05(4) Å^3	561.65(3) Å
Z	4	3	3
Density (calculated)	4.850 g/cm^3	4.495 g/cm^3	4.506 g/cm^3
Absorption coefficient	11.391	10.136 mm^{-1}	10.162 mm^{-1}
F(000)	856.0	672.0	
Radiation	Mo Kα (λ = 0.71073 Å)	Mo Kα (λ = 0.71073 Å)	Mo Kα (λ = 0.71073 Å)
Theta range for data collection	4.938 to 55.08 °	6.874 to 54.832 °	
Index ranges	$-6 \le h \le 6$, $-14 \le k \le 14$, $-15 \le l \le 15$	$-15 \le h \le 15$, $-15 \le k \le 15$, $-5 \le l \le 5$	
Reflections collected	12626	3648	13174
Independent reflections	1480 [*R(int)* = 0.0298, *R(sigma)* = 0.0155]	575 [*R(int)* = 0.0613, *R(sigma)* = 0.0321]	739 [*R(int)* = 0.0283, *R(sigma)* = 0. 0106]
Completeness to theta	96.2 % (27.54 °)	100.00 % (27.416 °)	
Refinement method	Full-matrix least-squares on F_o^2	Full-matrix least-squares on F_o^2	
Goodness-of-fit on F_o^2	1.184	1.076	1.225
Final R indices [I>2sigma(I)][#2]	R_1 = 0.0177, wR_2 = 0.0366	R_1 = 0.0178, wR_2 = 0.0398	R_1 = 0.0095, wR_2 = 0.0235
R indices (all data)	R_1 = 0.0184, wR_2 = 0.0369	R_1 = 0.0186, wR_2 = 0.0405	R_1 = 0.0095, wR_2 = 0.025
Largest diff. peak and hole	0.59 and -0.54 e/Å^3	0.52 and -0.55 e/Å^3	0.514 and -0.464 e/Å^3

[#1] This crystal data was reported by E. Uglova. (E. Uglova, M. Reichelt, H. Reuter, Formation and structural characterization of the basic tin(II) fluoride, $Sn_9F_{13}O(OH)_3{\cdot}2H_2O$, containing the unprecedented $[Sn_4O(OH)_3]^{3+}$ cage-ion, *Z. Anorg. Allg. Chem.* 2022, 648, e202200302.)

[#2] $R_1 = \Sigma||F_o| - |F_c||/\Sigma|F_o|$ and $wR_2 = [\Sigma w(F_o^2 - F_c^2)^2 / \Sigma wF_o^4]^{1/2}$ for $F_o^2 > 2\sigma(F_o^2$

Table S2. Selected bond lengths [Å] and angles [deg] for $[Sn_3OF]PO_4$ and $[Sn_3F_3]PO_4$.

$[Sn_3OF]PO_4$			
Sn(1)-O(2)$^{\#1}$	2.156(3) Å	Sn(3)-F(1)	2.260(2) Å
Sn(1)-O(4)	2.141(3) Å	P(1)-O(1)	1.559(3) Å
Sn(1)-O(5)	2.115(2) Å	P(1)-O(2)	1.541(3) Å
Sn(1)-F(1)$^{\#2}$	2.678(2) Å	P(1)-O(3)	1.532(3) Å
Sn(2)-O(1)$^{\#3}$	2.461(3) Å	P(1)-O(4)	1.534(3) Å
Sn(2)-O(1)$^{\#4}$	2.168(2) Å	O(2)-P(1)-O(1)	109.35(15) °
Sn(2)-O(5)	2.066(2) Å	O(3)-P(1)-O(1)	106.52(14) °
Sn(2)-F(1)	2.283(2) Å	O(3)-P(1)-O(2)	109.66(15) °
Sn(3)-O(3)	2.173(2) Å	O(3)-P(1)-O(4)	112.71(15) °
Sn(3)-O(5)	2.075(3) Å	O(4)-P(1)-O(1)	108.02(15) °
Sn(3)-O(2)$^{\#1}$	2.740(3) Å	O(4)-P(1)-O(2)	110.45(16) °
$[Sn_3F_3]PO_4$			
Sn(1)-O(1)	2.098(6) Å	P(1)-O(2)	1.556(10) Å
Sn(1)-O(2)$^{\#5}$	2.567(6) Å	O(1)$^{\#7}$-P(1)-O(1)$^{\#8}$	111.5(2) °
Sn(1)-F(1)	2.058(5) Å	O(1)-P(1)-O(1)$^{\#8}$	111.5(2) °
Sn(1)-F(1)$^{\#6}$	2.264(5) Å	O(1)$^{\#7}$-P(1)-O(2)	107.4(2) °
P(1)-O(1)	1.523(6) Å	O(1)-P(1)-O(2)	107.4(2) °
P(1)-O(1)$^{\#7}$	1.523(6) Å	O(1)$^{\#8}$-P(1)-O(2)	107.4(2) °
P(1)-O(1)$^{\#8}$	1.523(6) Å		

Symmetry transformations used to generate equivalent atoms:
$^{\#1}$ 1+*x*, *y*, *z*; $^{\#2}$ 1/2+*x*, 3/2-*y*, -1/2+*z*; $^{\#3}$ 3/2-*x*, 1/2+*y*, 1/2-*z*; $^{\#4}$ 1/2+*x*, 3/2-*y*, 1/2+*z*; $^{\#5}$ *x*, *y*, -1+*z*; $^{\#6}$ 5/3-*y*, 1/3+*x*-*y*, 1/3+*z*; $^{\#7}$ 1+*y*-*x*, 1-*x*, +*z*; $^{\#8}$ 1-*y*, +*x*-*y*, +*z*

Table S3. Atomic coordinates, Wycoff positions, equivalent isotropic displacement parameter and bond valence sum (BVS) for $[Sn_3OF]PO_4$ and $[Sn_3F_3]PO_4$.

	Atom	Wycoff	x	y	z	U_{eq}[#1]	BVS[#2]
$[Sn_3OF]PO_4$	Sn(1)	4*e*	11223.1(5)	8608.1(2)	2015.0(2)	15.65(8)	2.118
	Sn(2)	4*e*	7189.7(5)	8965.3(2)	4388.9(2)	16.24(8)	2.063
	Sn(3)	4*e*	10904.9(5)	6423.0(2)	4136.3(2)	18.64(8)	1.993
	P(1)	4*e*	6165.6(17)	6568.4(8)	1861.4(7)	12.17(17)	4.918
	O(1)	4*e*	5074(5)	5723(2)	887(2)	17.9(5)	2.053
	O(2)	4*e*	3707(5)	7069(2)	2395(2)	20.4(5)	1.984
	O(3)	4*e*	7985(5)	5836(2)	2731(2)	17.7(5)	1.867
	O(4)	4*e*	7765(5)	7554(2)	1366(2)	21.1(5)	1.985
	O(5)	4*e*	10202(5)	8137(2)	3616(2)	17.2(5)	2.287
	F(1)	4*e*	7309(5)	7068(2)	4979.1(19)	22.9(5)	0.915
$[Sn_3F_3]PO_4$	Sn(1)	9*b*	9052.0(5)	4506.6(6)	1048(3)	20.65(17)	2.114
	P(1)	3*a*	6666.67	3333.33	6015(7)	15.0(7)	5.042
	O(1)	9*b*	8081(6)	4103(8)	5033(12)	28.2(15)	2.096
	O(2)	3*a*	6666.67	3333.33	9380(20)	21(2)	1.796
	F(1)	9*b*	8669(6)	6010(5)	578(13)	39.2(15)	1.102

[#1] U_{eq} is defined as one-third of the trace of the orthogonalized U_{ij} tensor.
[#2] Bond valence sums are calculated by using bond-valence theory ($S_i = \exp[(R_o - R_i)/B]$, where R_o is an empirical constant, R_i is the length of bond I (in angstroms), and $B = 0.37$).

Table S4. Calculation detail of the contribution for $[Sn_3OF]PO_4$ and $[Sn_3F_3]PO_4$.

	Sn-centered Polyhedron in unit cell	Coordinate			Projected value(n_x)	Projected value(n_y)	Projected value(n_z)	Contribution of n_x	Contribution of n_y	Contribution of n_z
$[Sn_3OF]PO_4$	$^{1\#}[Sn(1)O_3F]^{5-}$	-0.14	0.12	-0.86	0.14	0.12	0.86	2.80	6.16	6.24
	$^{2\#}[Sn(1)O_3F]^{5-}$	-0.14	0.12	0.86	0.14	0.12	0.86			
	$^{3\#}[Sn(1)O_3F]^{5-}$	0.14	-0.12	-0.86	0.14	0.12	0.86			
	$^{4\#}[Sn(1)O_3F]^{5-}$	0.14	-0.12	0.86	0.14	0.12	0.86			
	∑Projected value(Sn(1))				0.56	0.48	3.44			
	$^{5\#}[Sn(2)O_3F]^{5-}$	-0.04	-0.86	-0.15	0.04	0.86	0.15			
	$^{6\#}[Sn(2)O_3F]^{5-}$	-0.04	-0.86	0.15	0.04	0.86	0.15			
	$^{7\#}[Sn(2)O_3F]^{5-}$	0.04	0.86	-0.15	0.04	0.86	0.15			
	$^{8\#}[Sn(2)O_3F]^{5-}$	0.04	0.86	0.15	0.04	0.86	0.15			
	∑Projected value(Sn(2))				0.16	3.44	0.60			
	$^{9\#}[Sn(3)O_3F]^{5-}$	-0.52	0.56	-0.55	0.52	0.56	0.55			
	$^{10\#}[Sn(3)O_3F]^{5-}$	-0.52	0.56	0.55	0.52	0.56	0.55			
	$^{11\#}[Sn(3)O_3F]^{5-}$	0.52	-0.56	-0.55	0.52	0.56	0.55			
	$^{12\#}[Sn(3)O_3F]^{5-}$	0.52	-0.56	0.55	0.52	0.56	0.55			
	∑Projected value(Sn(3))				2.08	2.24	2.20			
	∑Projected value(Sn)				2.80	6.16	6.24			
	Sn-centered Polyhedron in unit cell	Coordinate			Projected value(n_a)	Projected value(n_b)	Projected value(n_c)	Contribution of $n_{ac\text{-plane}}$	Contribution of $n_{\text{perpendicular to the } ac\text{-plane}}$	
$[Sn_3F_3]PO_4$	$^{1\#}[SnO_2F_2]^{4-}$	0.51	-0.33	-0.44	0.51	0.33	0.44	5.46	4.29	
	$^{2\#}[SnO_2F_2]^{4-}$	-0.84	-0.51	-0.44	0.84	0.51	0.44			
	$^{3\#}[SnO_2F_2]^{4-}$	0.33	0.84	-0.44	0.33	0.84	0.44			
	$^{4\#}[SnO_2F_2]^{4-}$	-0.84	-0.51	-0.44	0.84	0.51	0.44			
	$^{5\#}[SnO_2F_2]^{4-}$	0.33	0.84	-0.44	0.33	0.84	0.44			
	$^{6\#}[SnO_2F_2]^{4-}$	0.51	-0.33	0.44	0.51	0.33	0.44			
	$^{7\#}[SnO_2F_2]^{4-}$	0.42	1.05	-0.55	0.42	1.05	0.55			
	$^{8\#}[SnO_2F_2]^{4-}$	0.63	-0.42	-0.55	0.63	0.42	0.55			
	$^{9\#}[SnO_2F_2]^{4-}$	-1.05	-0.63	-0.55	1.05	0.63	0.55			
	∑Projected value				5.46	5.46	4.29			

Table S5. Calculation detail of the assessment of consistency arrangement for $[Sn_3OF]PO_4$ and $[Sn_3F_3]PO_4$.

	θ_i	n	$\frac{\sum_i^n cos\theta_i}{n}$
$[Sn_3OF]PO_4$	87.6 ° ×8 72.8 ° ×8 72.5 ° ×4 65.6 ° ×8 63.3 ° ×8 49.2 ° ×8 41.9 ° ×8 23.8 ° ×4 19.8 ° ×3 0 ° ×7	66	0.54
	θ_i	n	$\frac{\sum_i^n cos\theta_i}{n}$
$[Sn_3F_3]PO_4$	61.8 ° ×27 0 ° ×9	36	0.47

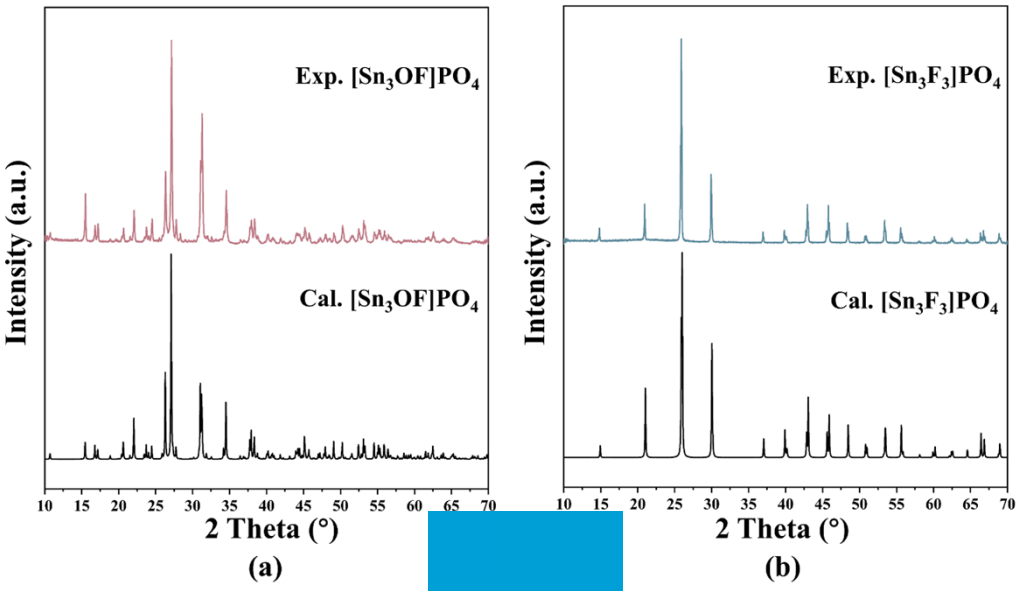

Figure S1. The XRD powder refined patterns of [Sn$_3$ PO$_4$.

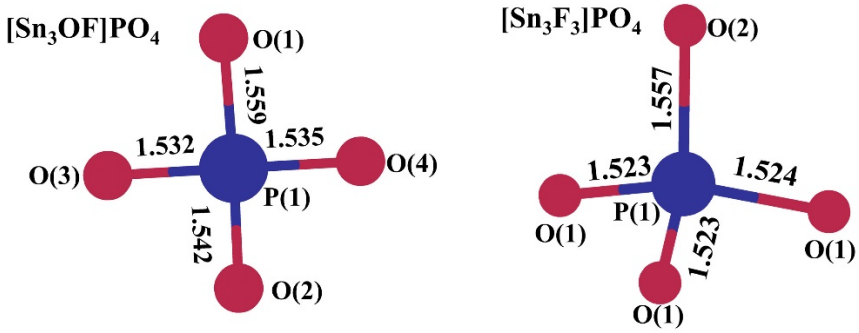

Figure S2. P-O bond length in $[PO_4]^{3-}$.

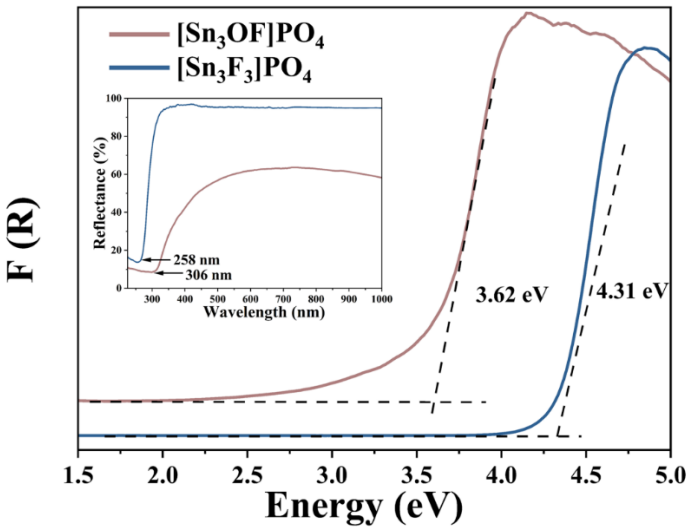

Figure S3. Experimental band gaps and UV-Vis diffuse reflection spectra of $[Sn_3OF]PO_4$ and $[Sn_3F_3]PO_4$.

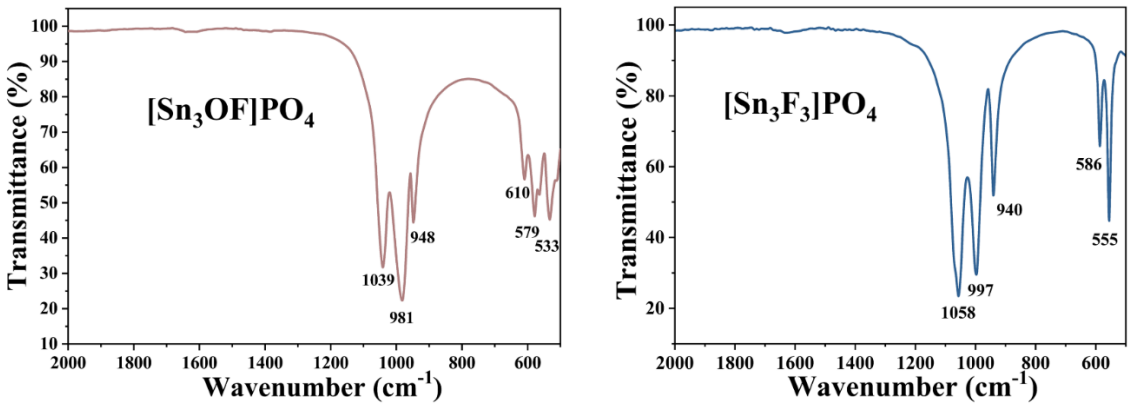

Figure S4. The IR spectra of $[Sn_3OF]PO_4$ and $[Sn_3F_3]PO_4$.

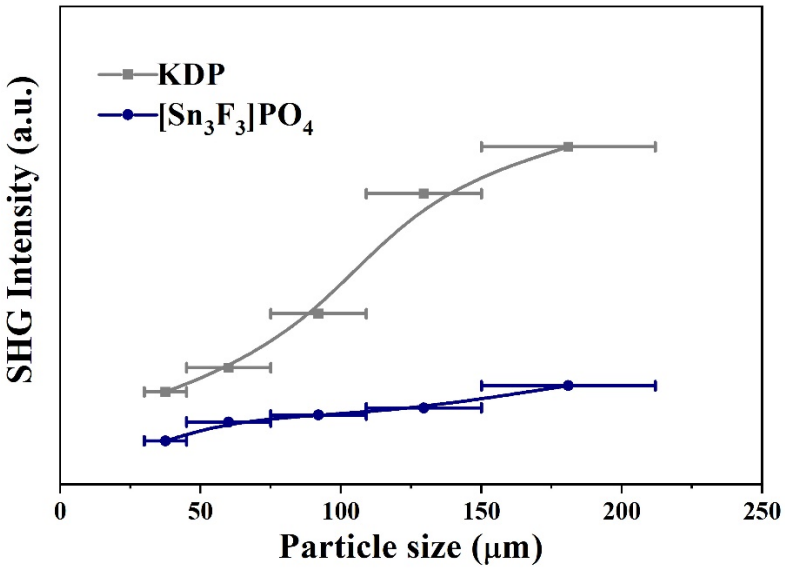

Figure S5. Powder SHG response of $[Sn_3F_3]PO_4$.

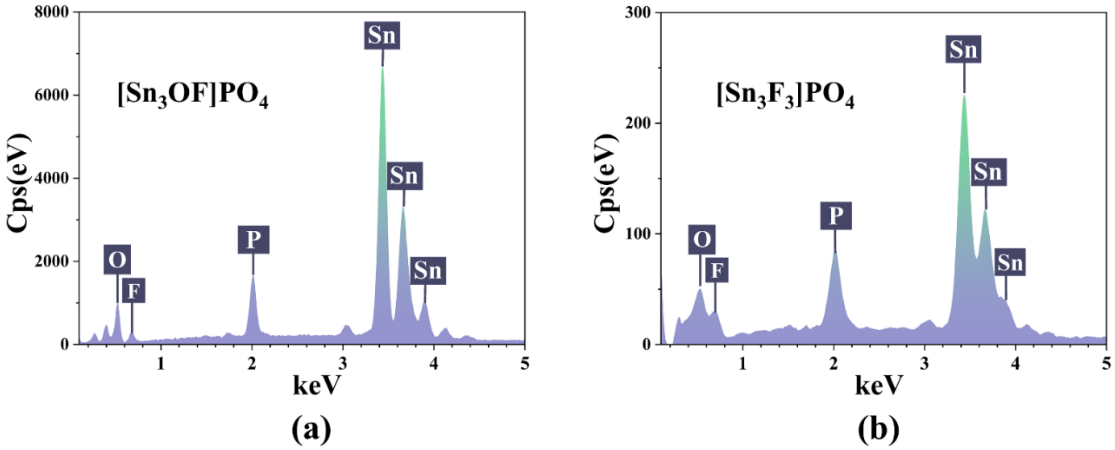

Figure S6. The EDS patterns of $[Sn_3OF]PO_4$ and $[Sn_3F_3]PO_4$.

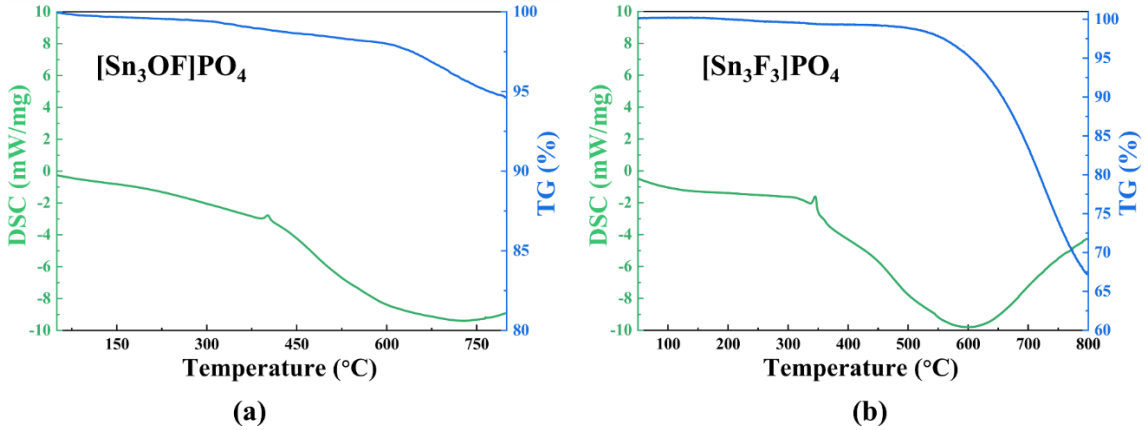

Figure S7. The TG-DSC of $[Sn_3OF]PO_4$ and $[Sn_3F_3]PO_4$.

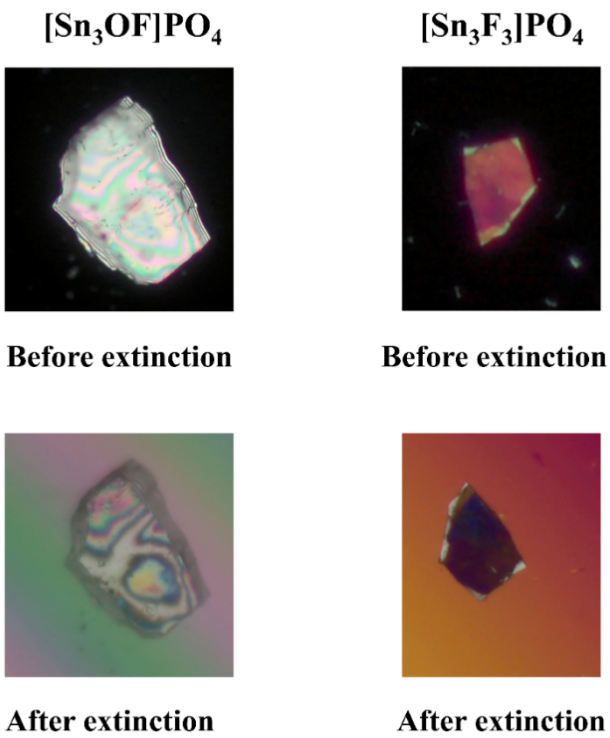

Figure S8. The crystals of $[Sn_3OF]PO_4$ and $[Sn_3F_3]PO_4$.

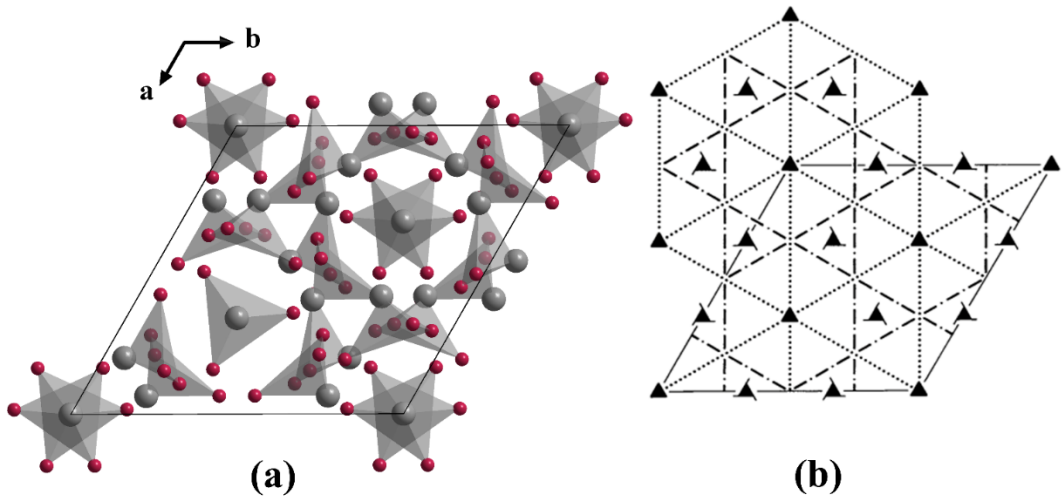

Figure S9. $NaSn_4(PO_4)_3$ viewed in the *ab* plane and the [001] projection of the symmetry elements of space group *R*3*c*.

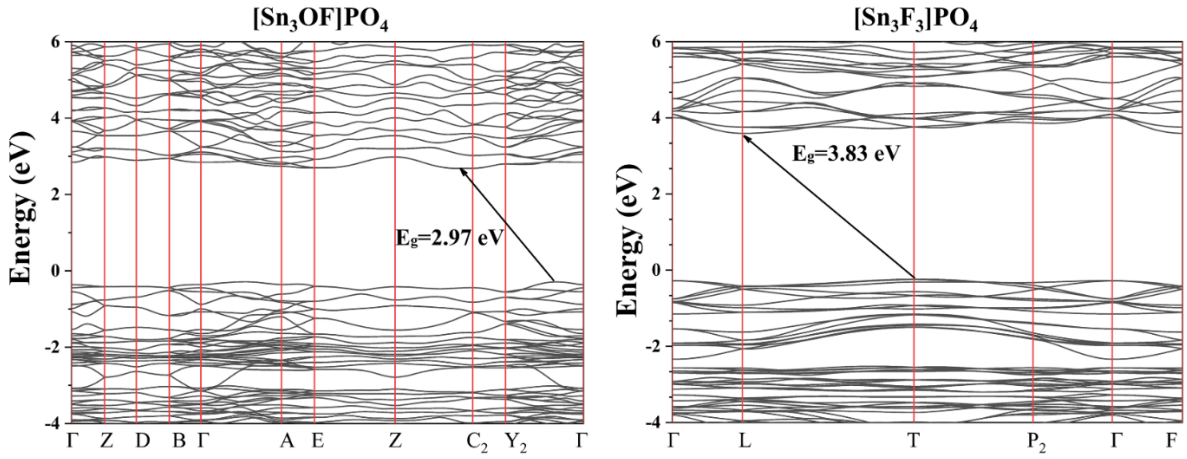

Figure S10. Calculated band gaps of $[Sn_3OF]PO_4$ and $[Sn_3F_3]PO_4$.

Reference

1 S.B. Etcheverry, G.E. Narda, M.C. Apella, E.J. Baran, Hydrolytic Properties of $Sn_3PO_4F_3$ (Short Communication), *Caries Res.*, 1986, **20**, 120–122.

2 S. K. Kurtz, T. T. Perry, A powder technique for the evaluation of nonlinear optical materials, *J. Appl. Phys.*, 1968, **39**, 3798−3813.